10.2174/1567201818666210402125244

Magnesium aluminium silicate-metformin hydrochloride complexes - The use of isothermal calorimetry in probing the understanding of clay and drug nanocomplexations

A.M. Totea[1], I. Dorin[2], P.R. Laity[3], B.R. Conway[1], L. Waters[1], K. Asare-Addo[1*]

[1]School of Applied Sciences, Department of Pharmacy, University of Huddersfield, Queensgate, Huddersfield, UK, HD1 3DH

[2]Biomolecular Formulation and Characterization Sciences, UCB, Slough SL3WE, UK

[3]Department of Materials Science and Engineering, University of Sheffield, Sir Robert Hadfield Building, Mappin Street, Sheffield, S1 3JD, UK

Corresponding author*

Dr Kofi Asare-Addo

Tel: +01484472360

Fax: +44 1484 472182

Submission: CDD

Orcid IDs:

P.R. Laity: 0000-0001-8608-875X

B.R. Conway: 0000-0001-5570-3318

L. Waters: 0000-0001-9172-0828

K. Asare-Addo: 0000-0001-6824-5336

Graphical Abstract

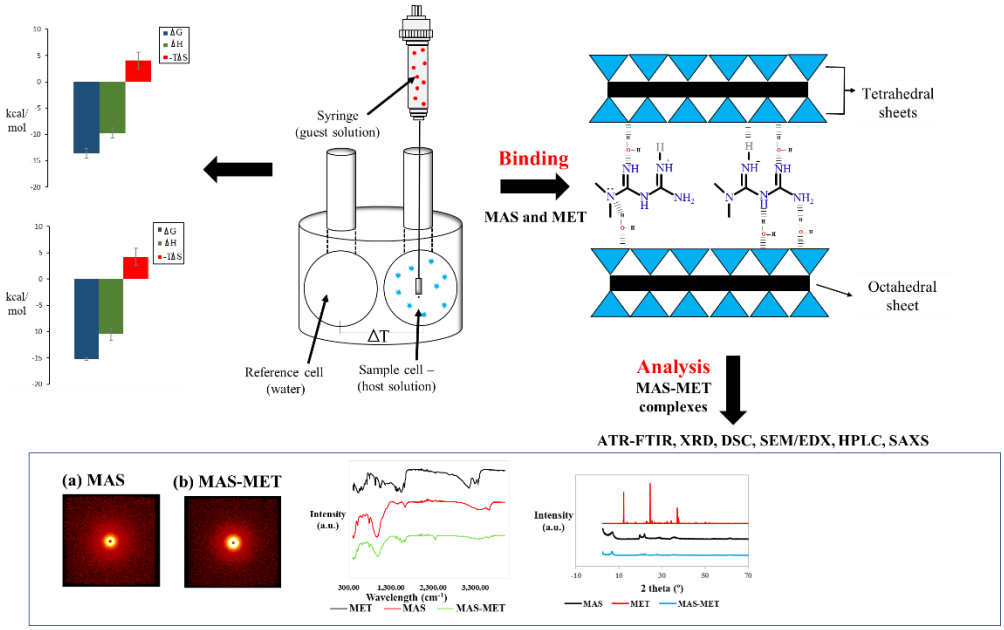

Highlights

MAS-MET complexes fully characterized up to nanometer scale.

XRPD analysis was inconclusive as a technique in distinguishing between MAS and its complexed particles with MET

2D-SAXS was used to distinguish complexed particles from MAS only particles in liquid state

SEM/EDX studies showed the occurrence of changes in the microstructural properties of MAS following complexation.

Thermodynamic studies showed that binding process between MET and MAS was enthalpy driven and entropically unfavourable.

Abstract

Background: Studying complexation between a wide variety of drugs and clay is of high importance in expanding the knowledge about controlled drug delivery and its exploitation. This study reports the use of isothermal calorimetry (ITC) in understanding the complexation process occurring between magnesium aluminium silicate (MAS) and metformin hydrochloride (MET), as a potentially controlled release drug delivery system.

Objectives: To fully characterise and understand the complexes formed between MAS and MET and how that might impact on controlled release systems.

Methods: MAS and MET complex dispersions and particles were formulated and analysed using ITC, DSC, XRPD, ATR-FTIR, SEM/EDX, digital microscopy and 2D-SAXS.

Results: The calorimetric results confirmed the binding between MET and MAS at various pHs (5, 7 and 9) and temperatures (25 ºC and 37 ºC). The overall change in enthalpy was found to be exothermic with a comparatively small entropic contribution to the total change in Gibbs free energy, implying that the binding was an enthalpically driven process. These findings suggest that the binding process was dominated by hydrogen bonding and electrostatic interactions. pH and temperature variation did not have a great impact on the binding, as observed from the similarity in enthalpy (ΔH), entropy (ΔS) or Gibbs free energy (ΔG), with the reaction being only slightly more exothermic at pH 5 and at 37 ºC. 2D-SAXS was able to differentiate between MAS particulates and MAS-MET complexes when analysed in their liquid form suggesting the importance of appropriate methodology and instrumentation used in characterisation.

Conclusion: ITC was successfully used in understanding the complexation process occurring between MAS and MET. Care and consideration however should thus be taken in the accurate determination and characterisation techniques for the formation of complexes for controlled release using MAS.

Keywords: isothermal titration calorimetry, magnesium aluminium silicate, metformin hydrochloride, single injection mode, multiple injection mode

Abbreviations: MAS, magnesium aluminium silicate; MET, metformin hydrochloride; ITC, isothermal titration calorimetry; SIM, single injection mode; MIM, multiple injection mode; HPLC, high performance liquid chromatography; RSD, relative standard deviation; ICH, International Conference on Harmonisation; LOD, limit of detection; LOQ, limit of quantification; HCl, hydrochloric acid; rpm, rotations per minute

1. Introduction

Minerals such as montmorillonite and saponite are widely used within the pharmaceutical industry as excipients within drug formulation. Such smectite clays have unique chemical composition but share structural similarities and are often used as disintegrants due to their high swelling capacity and acid-absorbing capacity, as diluents and binders due to their plasticity, as emulsifying, thickening and anticaking agents due to their colloidal and thixotropic properties and as flavour correctors due to their high sorption capacity. However, recent studies published in literature focus on the ability of smectite clays to interact or form complexes with cationic drugs to control drug release.[1]–[8] Some of these studies also explore the efficiency of clay-drug complexes combined with a variety of polymers in controlling drug release, assessing therefore a complex drug delivery system.

Magnesium aluminium silicate (MAS) (*Veegum*®) is a mixture of natural smectite montmorillonite and saponite clays. MAS is formed of one alumina or magnesia octahedral sheet, sandwiched between two tetrahedral silicate sheets (Fig. 1).[9] When Al^{3+} is the predominant cation, as in montmorillonite, only two of every three octahedral positions are occupied in order to maintain the charge balance within the clay lattice (dioctahedral clay). In contrast, all octahedral positions are filled when the central cation is Mg^{2+}, as in saponite (trioctahedral clay).[10] A single MAS platelet is 0.96 nm thick and up to several hundred nm across.[11]

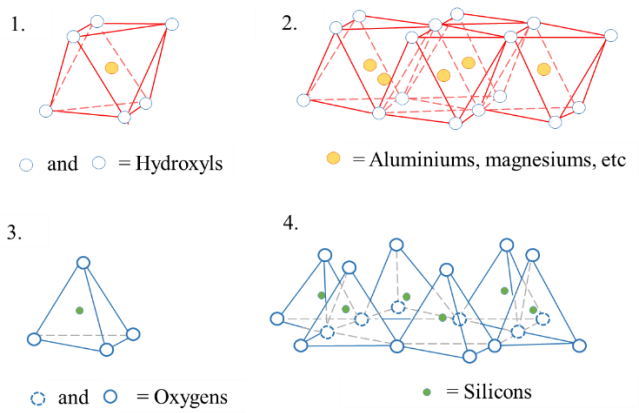

Fig 1. (1.) Alumina octahedron; (2.) Alumina sheet composed of alumina octahedron structures joined together; (3.) Silica tetrahedron; (4.) Silica sheet composed of silica tetrahedron structures joined together; octahedral sheet, sandwiched between two tetrahedral silicate sheets make up the structure of montmorillonite and saponite clay minerals: adapted from [10]

Metformin hydrochloride (MET) (Table 1) is an orally administered biguanide that was firstly clinically used in 1958.[12], [13] It represents the first choice of treatment for type 2 diabetes mellitus (non-insulin dependent diabetes mellitus), being highly prescribed worldwide.[14] MET promotes glycaemic control by reducing the hepatic glucose production and the intestinal glucose absorption and by improving glucose uptake and utilisation.[14] MET also has additional health benefits such as reduction of body weight, decrease of blood plasma lipid levels, as well as prevention of cardiovascular complications.[14], [15]

Table 1. Chemical structure and physicochemical properties of metformin hydrochloride

Structure	**MW**	**pK_a**
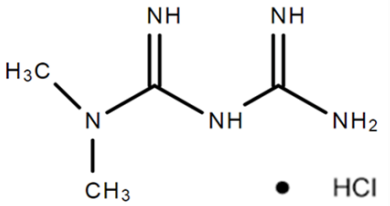	165.63	3.0 ± 1.0 11.9 ± 0.4

Despite its therapeutic benefits, MET has a short plasma half-life of 1.5 – 4.5 h, requiring administration of 250 mg 2 – 3 times a day when larger doses are required, as well as a low absolute bioavailability of 50 – 60 %.[12] Therefore, to maintain adequate drug plasma levels and hence prolong its therapeutic effects, sustained release formulations are required.[14], [16] The present study aims to understand and fully characterise the complexes that are formed

between magnesium aluminium silicate (MAS) and metformin hydrochloride (MET) using techniques such as isothermal calorimetry and small angle X-ray scattering. The aim is therefore to also understand how these complexed particles can be exploited as a potential controlled drug delivery system where MAS becomes a carrier for the MET. Previous studies by Totea et. al. and Pongjanyakul et. al. characterised and demonstrated the efficiency of drug-clay complexes to control the release of propranolol and diltiazem.[1], [2], [4], [6], [17] Studying complexation between a wide variety of drugs and clay is of high importance in expanding the knowledge about controlled drug delivery and its exploitation.

2. Experimental

2.1. Materials

Veegum F EP® (magnesium aluminium silicate) was a gift from R.T. Vanderbilt Company, Norwalk, CT (USA). This material complies with the European Pharmacopoeia monograph for magnesium aluminium silicate and is indicated for use as a dry excipient in pressed powders and in direct compression tablets.[18] Its composition was previously reported in literature.[1] Metformin hydrochloride (MET) was supplied from TCI (Tokyo Chemical Industry, Tokyo). Acetonitrile (HPLC grade), sodium phosphate dibasic dihydrate, 99+% (HPLC grade), 2 N sodium hydroxide and 2N hydrochloric acid were purchased from Fisher Scientific (UK).

2.2. Methods

2.2.1. Formulation of MAS-MET complex particles

Drug solution of MET (2 % w/v) and MAS dispersion (2 % w/v) were separately prepared under continuous stirring for 24 h, at 25 ºC and 500 rpm. The pH of MAS dispersion and MET solution prepared was further adjusted to pH 5 using using 2 M hydrochloric acid or 2 M sodium hydroxide. For the first drug loading, MAS dispersion and MET solution prepared were

combined, and the obtained flocculated complex dispersion was incubated at 37 °C with shaking at 200 rpm for 24 h (GLS Aqua 18 Plus, Linear Shaking Water Bath, Grant Instruments). After 24 h, the complexes were filtered using a Buchner filtration apparatus. For the second drug loading, the single drug loaded flocculates previously obtained were redispersed into a fresh MET solution (2 % w/v) and the double drug loaded complex dispersion obtained (Fig. 2) was further incubated at 37 °C with shaking for 24 h. The double drug loaded MAS–MET flocculated complexes obtained were filtered and dried in the oven at 50 ºC for 48 hours. The final double drug loaded MAS-MET complex particles obtained were ground using a Retsch® PM 100 Ball Mill set at 350 rpm for 10 min, until fine powder was obtained and sieved to collect the particle size fraction between 65 – 123 µm. The samples were stored in sealed glass vials until required.

Fig 2. MAS-drug flocculated complex dispersion

2.2.2. Characterisation of MAS-MET complexes

2.2.2.1. Attenuated total reflectance Fourier transform infrared spectroscopy (ATR-FTIR)

Infrared spectroscopy represents a powerful qualitative and quantitative analytical technique that can detect changes in the unique vibrational spectrum of a molecule. Hence, it can provide information about the chemistry of samples.[19] The technique was used to elucidate the

molecular interaction between MAS and MET. Experiments were performed on a Smart Orbit ATR-FTIR machine, using diamond as the ATR crystal. MAS, MET and dried MAS-MET complexes were scanned from 4000 to 400 cm^{-1}.

2.2.2.2. Powder X-ray diffractometry (PXRD)

Experiments were performed on a D2 PHASER XRPD from BRUKER and sample preparation involved the placement of MAS, MET and MAS-MET complexes in powder form onto a transmitter holder. Analysis was performed at an angular range of 2.5 - 40° (2θ) and a step angle of 0.02 ° (2θ) s^{-1}. The X-ray source was generated as a Cu radiation at 30 kV and 10 mA. Bragg's Law (Equation 1) was used to calculate the basal spacing by the approximation of the *001* plane peak (basal distance).[3]

$$n\lambda = 2d\sin\theta \qquad \textbf{Equation 1}$$

where $n = 1$

2.2.2.3. Differential scanning calorimetry (DSC)

DSC was used to study the thermal behaviour of MAS, MET and the MAS-MET complexes. Sample powder (less than 10 mg) was added onto a 40 µL aluminium crucible with the lid hermetically sealed. The measurements were performed between 25 and 500 °C, at a rate of 10 °C/min.

2.2.2.4. Scanning electron microscopy (SEM) with energy dispersive X-ray spectroscopy (EDX)

A QUANTA FEG 250 microscope equipped with EDX was used to study the surface morphology in 3-D and the energy spectrum of MAS, MET and MAS-MET complexes. The

electronic beam voltage of the microscope was set at 20 kV and the working distance was 30 mm. Sample preparation involved placement of the material particles in powder form onto a sample holder, and then coating their surface in a thin layer of gold (1 – 5 nm).

2.2.2.5. Microscopy

The morphology of the formulated flocculated MAS-MET complexes (formulated as described in section 2.2.1.) was analysed under a light microscope (Leica) at different magnifications. Sample preparation involved pipetting and spreading evenly a few drops of flocculated MAS-drug complex dispersions onto a glass slide.

2.2.2.6. Small Angle X-Ray Scattering (SAXS)

SAXS was used to study the morphological changes of MAS upon the formation of flocculates following the adsorption of MET onto MAS, as well as to analyse the morphological characteristics of the MAS and the formed MAS-MET complexes in the solid-state form. This was conducted as reported in Totea et al.[6]

Solid state analysis was performed on MAS and MAS-MET double drug loaded complexes (particle size 63-125 µm). Samples were placed in disposable borosilicate glass capillary tubes (diameter 2.0 mm) and sealed at both ends. 2D-SAXS patterns were collected for all the samples and for the background using an acquisition time of 1000 sec. Transmission was calculated using a glassy carbon filter to correct for the probability of sample absorption using Equation 2.

$$t = \frac{I_{X+GC} - t_{GC} \cdot I_X}{I_{GC} - t_{GC} \cdot I_0} \qquad \textbf{Equation 2}$$

where t_{GC} is glassy carbon filter transmission, I_X is the number of counts collected from sample, I_{X+GC} is the number of counts from sample with glassy carbon filter, I_{GC} is the number of counts with glassy carbon filter and I_0 is the number of counts from empty chamber.

Liquid-state analysis was performed on the MAS dispersion and MAS-MET flocculated complexes. Small samples (approx. 100 µL) were carefully pipetted in a metal cell fitted with a glass capillary, having a 1 mm diameter. Nanography was used to determine the coordinates of the sample holder. Data acquisition time was 1000 s and the background scattering (i.e. ultra-pure water at pH 5) was subtracted from each sample prior to data analysis.

2.2.3. Drug content analysis from MAS-MET complexes

Drug content was determined by dispersing 50 mg of the double drug loaded MAS-MET complex particles (in powder form) in 100 mL of 2 M HCl, ultra–pure water or pH 6.8 phosphate buffer under continuous stirring for 24 h, at 25 °C and 700 rpm. The dispersions obtained were filtered using 0.2 µm syringe filters and the filtrate obtained was then assessed using HPLC to determine the MET content. Experiments were performed in triplicate to ensure reproducibility.

2.2.4. High Performance Liquid Chromatography (HPLC)

High performance liquid chromatography was performed on a Shimadzu HPLC system equipped with an auto sampler. The column chosen was an XTerra® MS C18 150 mm × 4.6 mm × 3.5 µm. The mobile phase was prepared using acetonitrile and 0.01 M disodium hydrogen orthophosphate (pH 3.5) at a ratio of 30:70 v/v respectively. The flow rate of the mobile phase was set at 1 mL/min and the UV detection was set at 233 nm. An appropriate

calibration curve was obtained with a 100 µg/mL MET standard stock solution with MET standard solutions at 75, 50, 40, 30, 20, 10, 5, 1 and 0.1 µg/mL in ultra-pure water.

2.2.5. Calorimetric binding studies

Calorimetric binding studies were carried out a VP-ITC micro calorimeter (Malvern Panalytical, UK) and calibrated to ensure its working within acceptable limits. Single injection binding experiments were carried out at 25 °C and at three different pH values, 5, 7 and 9 to characterise the process of adsorption of MET onto MAS and identify the most favourable media for the reaction. Separate MAS dispersions and MET solutions were prepared separately using purified water under continuous stirring at 500 rpm at 25 ºC for 24 h and 30 min respectively prior to the analysis. The pH of the prepared solutions and dispersions was further adjusted to 5, 7 and 9. Each of the drug solutions prepared was separately added in one 150 – 250 µL injection into the sample cell containing MAS. The single injection mode allowed for fast titration experiments compared to the conventional experiments and gave an indication of the binding isotherm in real time.[20]

Multiple injection binding experiments were carried out at pH 5 and at two different temperatures (25 °C and 37 °C). The instrument was used in high-gain feedback mode, applying a reference power of 20 µcal s^{-1} whilst stirring its contents at 307 rpm. The real-time binding isotherm was studied in 29 injections of 10 µL each into the sample cell every 500 s. MAS dispersions and drug solutions were prepared under continuous stirring also. A mathematical model was then fitted to the data using Origin 7.0 software to get thermodynamic parameters which best reproduce the experimental data. Data produced from the blank titrations was subtracted from the sample titration so that that the dilution heat reflected only the interaction of interest. Experiments were repeated in triplicate to ensure reproducibility.

3. Results and discussion

3.1. Microscopy images of flocculated MAS-MET samples

The observation of the MAS-MET flocculates under light microscope showed that upon the addition of the MET solution to the MAS dispersion, flocculates formed which were shown to be aggregated in large clusters (Fig. 3). MAS dispersion in water was previously analysed using microscopy by A. M. Totea *et al*. and was shown to be formed of monodispersed particles.[2] This outlines the effects on MAS dispersion stability upon MET solution addition, which is consistent with the observations reported by A. M. Totea *et al*. following diltiazem hydrochloride (DIL) solution addition to MAS dispersion. This flocculation that occurs with the addition of drug is confirmation of the complexation process.

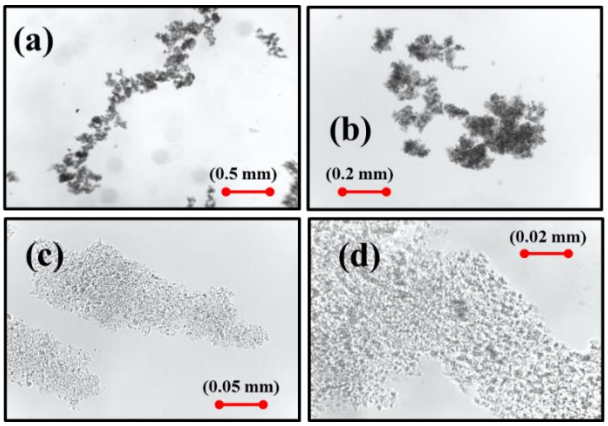

Fig 3. Microscopy images of MAS-MET complex dispersion prepared using purified water (pH 5) at different magnifications: × 4 (a); × 10 (b); × 40 (c); and × 100 (d)

3.2. Attenuated total reflectance Fourier transform infrared spectroscopy (ATR-FTIR)

The analysis of the spectrum belonging to MET (Fig. 4) showed peaks in the region 1000-1200 cm^{-1} representing stretching vibration of the C-N group.[21] Peaks in the region 1565 – 1400 cm^{-1} can be attributed to the asymmetric deformation of CH_3 groups and N-H in-plane deformation.[22] The adsorption bands observed at 1622 and 1580 have been linked to the fact that MET is a biguanide, corresponding to the C=N stretching vibration, whereas peaks

observed at 3145, 3292 and 3370 cm^{-1} can be assigned to the symmetric and asymmetric N-H stretching vibrations.[21], [22] The analysis of the MAS-MET complex particles showed structural differences compared to the MET and MAS spectrums. The presence of the Si-O-Si stretching at 980 cm^{-1}, as well as the peak showing the hydroxyl stretching belonging to Si-OH stretching at approximately 3625 cm^{-1}. Both belong to the MAS and were still observed on the spectrums of MAS-MET complex particles (Fig. 4). The sharp peak at 1640 cm^{-1} belonging to the hydroxyl group bending of water of crystallization onto the MAS was also observed.[3] The peaks observed at 1580 belonging to MET C=N stretching vibration were observed on the spectrums of MAS-MET complex particles, whilst the peaks assigned to the N-H stretching vibrations changed as MET is expected to be adsorbed onto MAS via hydrogen bonds formation between the silanol groups of MAS with the amine groups of MET. Subtle changes in the O-H stretching peak at 3625 cm^{-1} and the O-H bending peak at 1640 cm^{-1} may potentially suggest that water bound with MET and/or MAS in the complexes via hydrogen bonding through the water bridging mechanism.[3], [23]

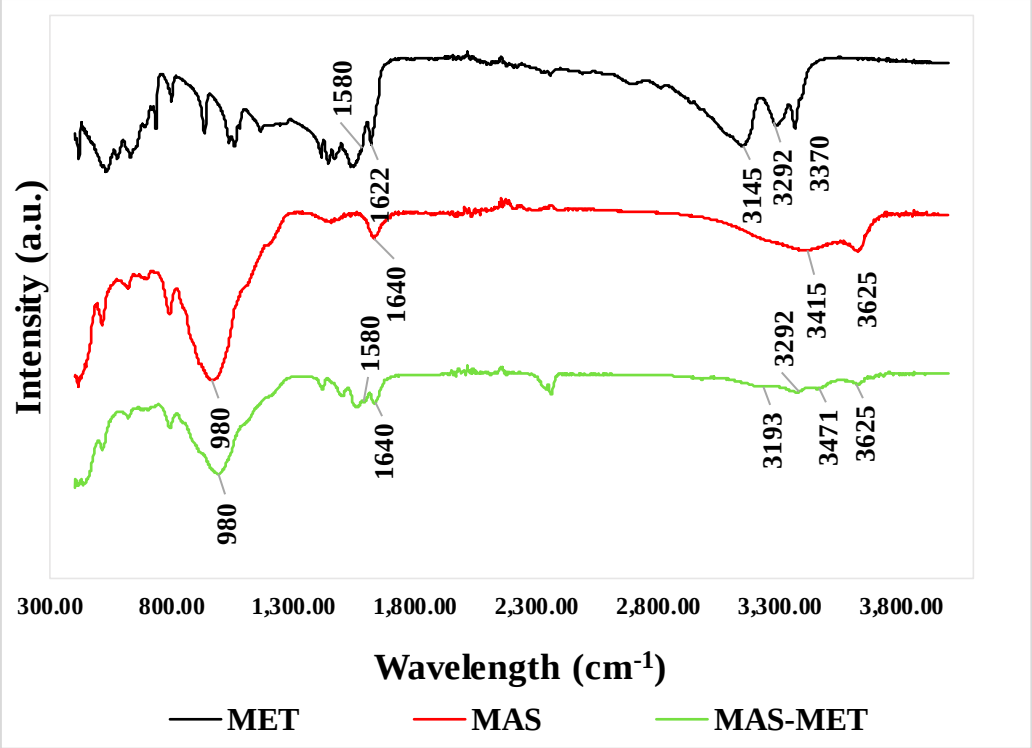

Fig 4. ATR-FTIR scans on MAS, MET and MAS-MET complex particles

3.3. Powder X-ray diffraction (PXRD)

Sharp, intense and representative diffraction peaks indicating the crystalline state of MET were observed at 2θ angles 12°, 24°and 37°.[24]–[26] The prepared MAS-MET complex particles did not follow the PXRD pattern of MET or MAS alone, suggesting the molecular dispersivity of the drug in the prepared complexes in its amorphous form (Fig. 5). The reflection at 6.87° (2θ) representing the thickness of the silicate layer in the MAS sample was observed in the diffractograms of the MAS-MET complexes prepared, although at a slightly different intensity. The changes in basal spacing upon MET adsorption onto MAS was hence calculated using Bragg's Law as 1.30 nm, suggesting no increase in basal spacing of MAS (1.28 nm). This was most probably due to the MAS-MET sample tested being well dried as opposed to the MAS since humidity is well known to affect basal spacing.

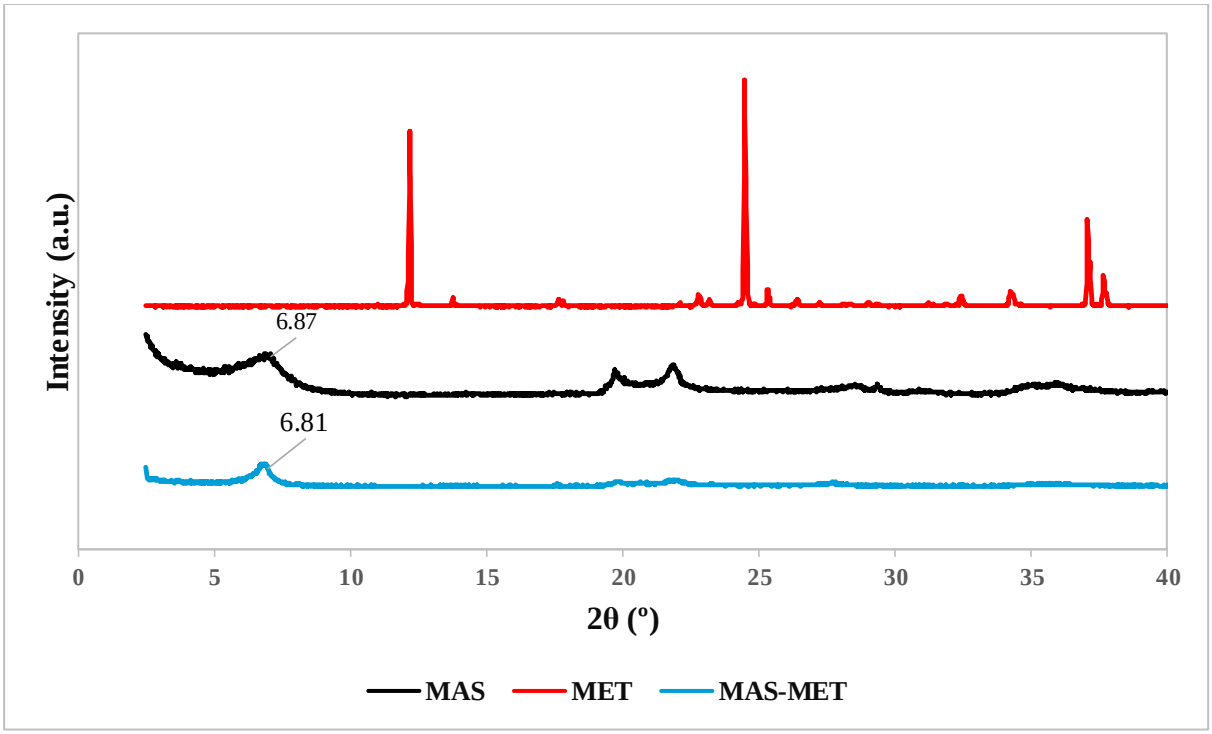

Fig 5. PXRD patterns of MAS, MET and MAS-MET complex particles

To test the sensitivity of the clay to humidity, further successive XRPD runs were performed on the MAS alone. Results demonstrated that dehydration and rehydration were responsible for basal distance variations, as a decrease in the distance between platelets from 1.30 to 1.22 nm following dehydration caused by the PXRD heating upon use was observed (Fig. 6). The sensitivity of clays to humidity as observed here using XRPD was in agreement to previously reported literature.[27], [28]

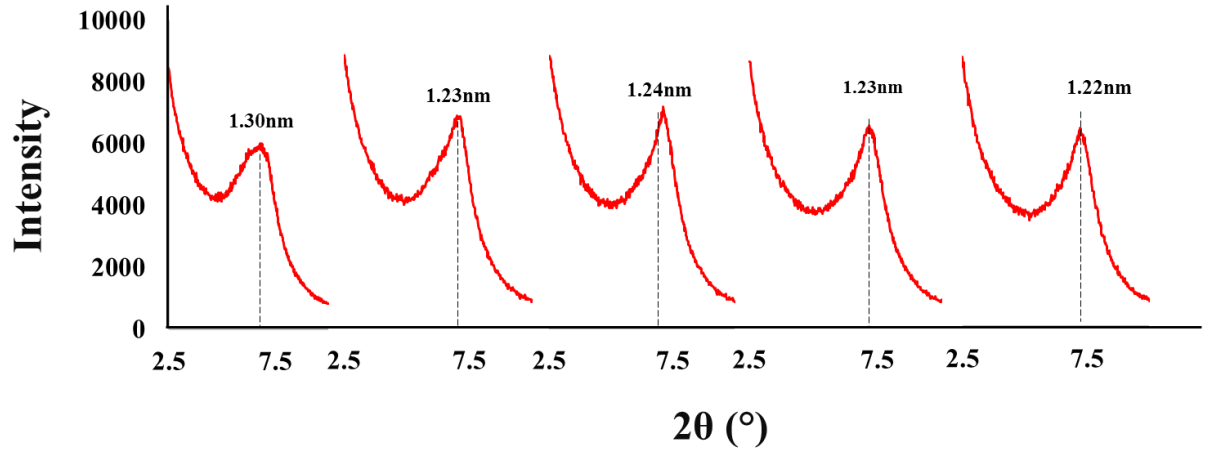

Fig 6. PXRD successive runs testing variations in basal distance of MAS following dehydration

The results hence suggest that an increase in basal distance may not accurately reflect the intercalation of a drug within clay platelets when humidity is not controlled to allow for comparisons.

3.4. Differential scanning calorimetry (DSC)

The melting point of MET was indicated by a sharp endothermic peak at 235.38 °C (Fig. 7).[26] The MAS thermogram showed the presence of a broad endothermic peak at 115°C that occurred following dehydration. The MAS-MET complexes were shown to be amorphous and the absence of MET melting point on their thermograms confirmed its molecular dispersion in amorphous form in the complexes (Fig. 7).

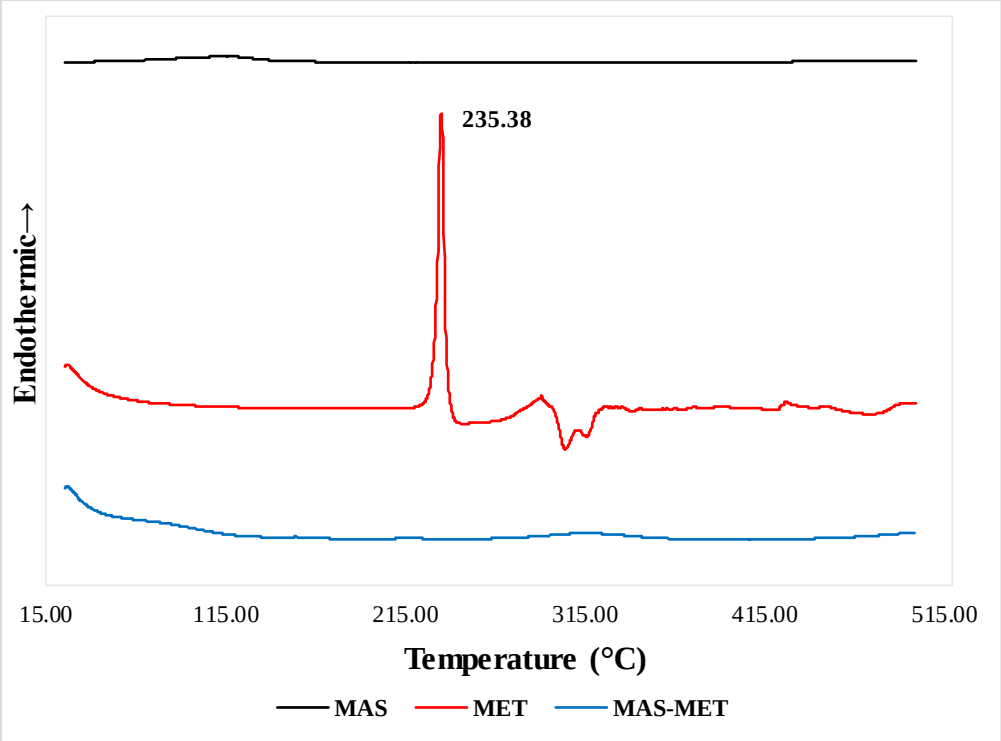

Fig 7. DSC thermogram of MAS, MET and MAS – MET complexes

3.5. Scanning electron microscopy (SEM) with energy dispersive X-ray spectroscopy (EDX)

MET, as well as the double drug loaded MAS-MET complex particles prepared were studied using SEM and EDX to understand their surface and the chemical elements existing in the samples. Due to the low sensitivity of the technique, the atomic distribution of elements varied and hence, chemical elements found in samples were not compared quantitatively.[29] MET crystals were shown to be large and on their surface, circular indents could be observed (Fig. 8). EDX analysis of MET confirmed the presence of distinctive elements such as chlorine and nitrogen in the tested specimen (Fig. 8).

(a)
(500 µm)
(b)
(100 µm)
(c)
(50 µm)
1
2
(10 µm)
Spectrum 1
Spectrum 2
Full Scale 33658 cts Cursor: 0.000
keV

345

346

Fig 8. Characterisation of MET surface using SEM/EDX. SEM images at different magnifications × 100 (a), × 500 (b), × 1000 (c) and × 5 000 (d); atomic distribution profile at two different sample locations (Spectrum 1 and 2)

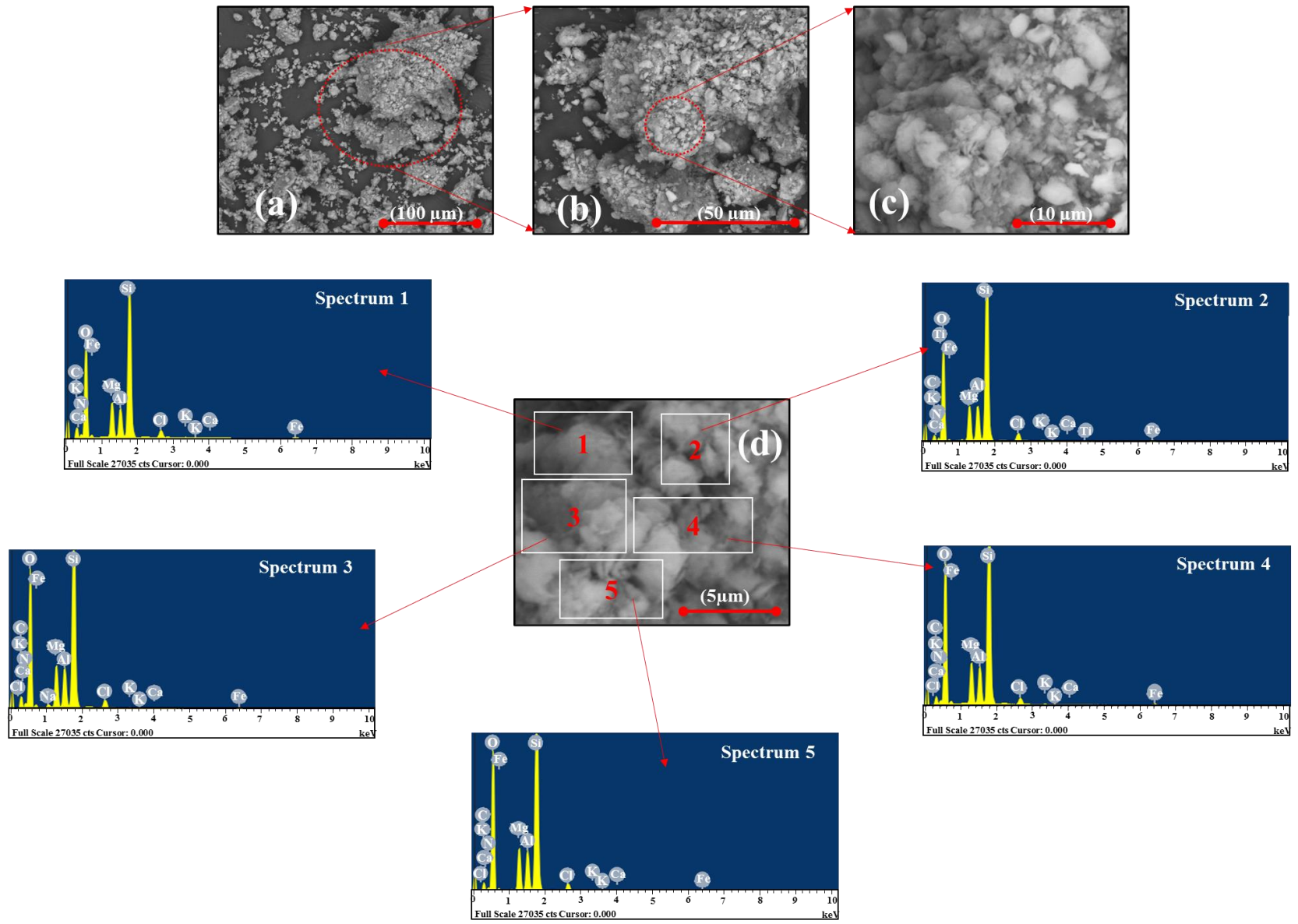
(a)
(100 µm)
(b)
(50 µm)
(c)
(10 µm)
Spectrum 1
Spectrum 2
Spectrum 3
Spectrum 4
Spectrum 5
1
2
3
4
5
(d)
(5µm)
Full Scale 27035 cts Cursor: 0.000
keV

Fig 9. Surface characterisation of MAS-MET complexes using SEM/EDX. SEM images at different magnifications ×500 (a), × 1500 (b), × 5000 (c) and ×10 000 (d); atomic distribution profile at five different sample locations (Spectrum 1-5)

MAS-MET complexes were shown to have an irregular layered surface (Fig. 9), very different to the MAS as reported by Totea *et. al*. 2019 or to the crystalline MET.[1] This demonstrates changes in the microstructural properties of the clay powder following the complexation process.[3]

3.6. Small angle X-ray scattering (SAXS)

3.6.1. Solid-state nanometre scale morphology

2D-SAXS data pattern for MAS and MAS-MET complexes was shown to be symmetric and circular, suggesting that at the nanometre scale, the particles showed no preferred orientation. This behaviour is due to the sample being analysed in its powder form, which implies randomly orientated particles. The intensity plot showing Log {I(a.u.)} vs. q [nm^{-1}] had a smooth curve, showing the intensity decreasing from $q \approx 0.099$ nm^{-1} (at $2\theta = 0.14^{o}$) at the edge of the beam stop, to $q = 2.275$ nm^{-1} (at $2\theta = 3.20^{o}$) at the peripheral limit of the detector. No peaks or other specific features were observed. Background subtraction was considered unnecessary due to the minimal background scattering in comparison to sample scattering intensity (Fig 10.) Data was corrected for transmission through the calculation on the transmission factor using glassy carbon, to correct for sample absorption.

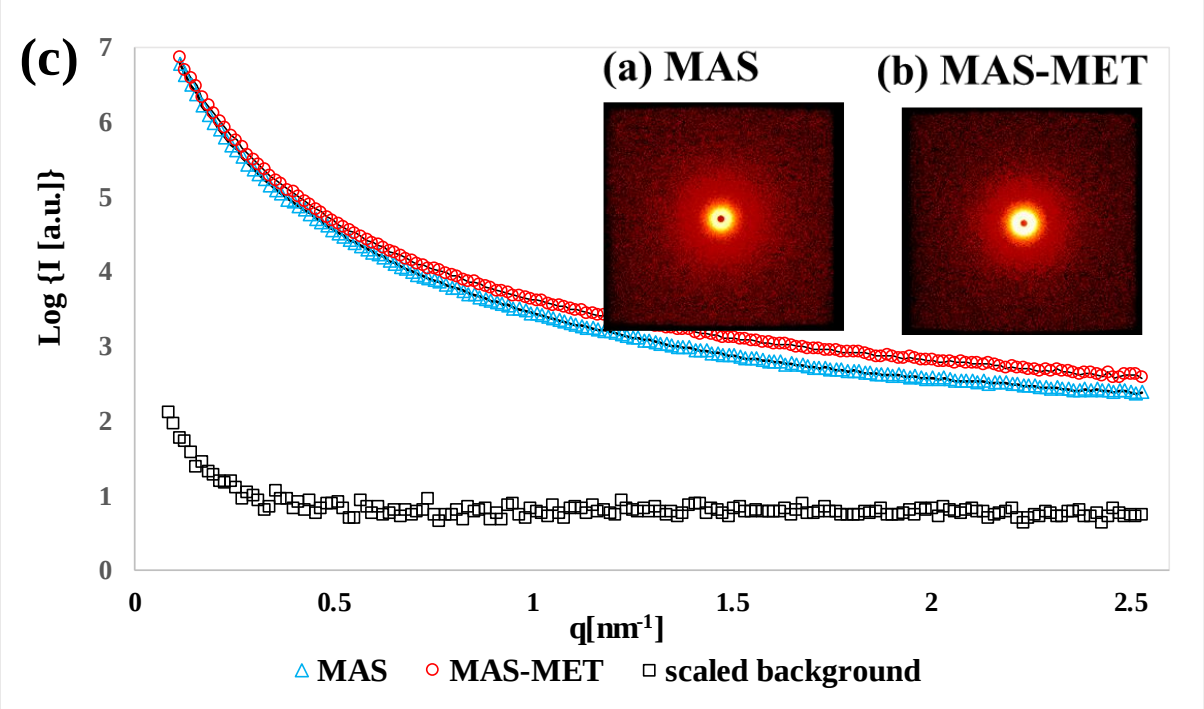

Fig 10. Typical SAXS data for specimens in powder form: (a and b) 2D-SAXS patterns for MAS and MAS-MET complexes showing the centre of the beam stop; (c) 1D-SAXS intensity curves for MAS and MAS-MET complexes (open symbols showing uncorrected data and line showing data after scaled background subtraction), and scaled background (open black square symbols)

The analysis of the data in the form of double logarithmic plot of intensity (log I [a.u.]) vs. the scattering vector (log {q [nm^{-1}]}) followed a straight line with no peaks or other specific features, indicate power-law scattering behaviour, similarly to the MAS powder behaviour (as described in a previously (Totea *et. al.* 2020). A slope of – 3.55 was obtained for the MAS-MET complexes, which was very similar to the slope obtained from the double logarithmic plot of intensity vs. the scattering vector for MAS (– 3.63) (Fig 11.).

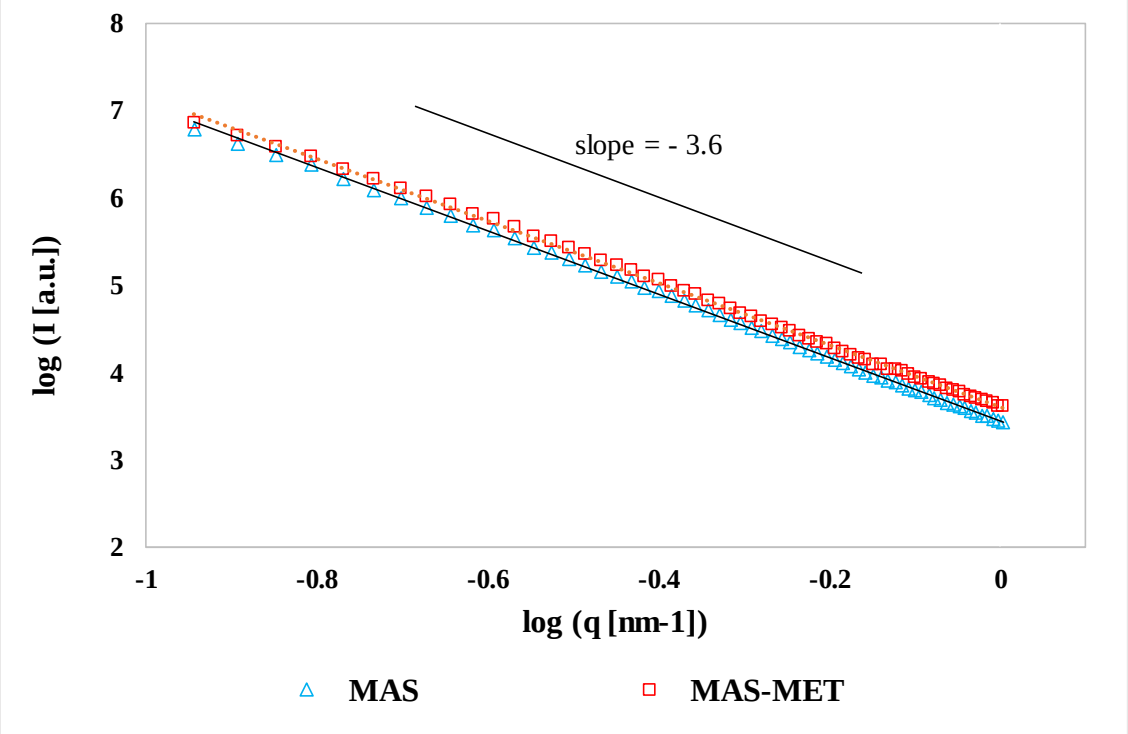

Fig 11. Double-logarithmic plot of intensity vs. the scattering vector for MAS and MAS-MET complexes in powder form (particle size 63 – 125 µm), showing the slope of the linear part for the data which allows the calculation of the power-law constant a as −3.63 for MAS and −3.57 for MAS-MET complexes

Slope determination from the double logarithmic plot of intensity vs. the scattering vector allowed for the calculation of the surface fractal dimension D_s value for MAS-MET complexes (Fig 11.). Hence, upon calculation, a surface fractal dimension D_s of 2.43 was obtained for MAS-MET complexes, suggesting that the sample tested was surface fractal over a length scale of 0.1 nm to 1.0 nm. The value also indicates an irregular, rough and space filling surface, and was very similar to the surface fractal dimension D_s value obtained for MAS (D_m = 2.37). The similarity of surface fractal dimension values between the samples (MAS compared to MAS-MET complexes) may create difficulties in differentiating between them, hence not being an indicator of drug absorption onto clay.

3.6.2. Liquid-state nanometre scale morphology

Data acquired from the flocculated complexes formed between MAS and MET and from the MAS also was represented using a Guinier plot (log(I) vs. q^2). The plot showed two linear regions separated by a transition region (Fig 12.), behaviour that suggests poly-dispersive systems in which cluster size is variable, with large cluster aggregates in the samples [30]. No peaks or other specific features were observed.

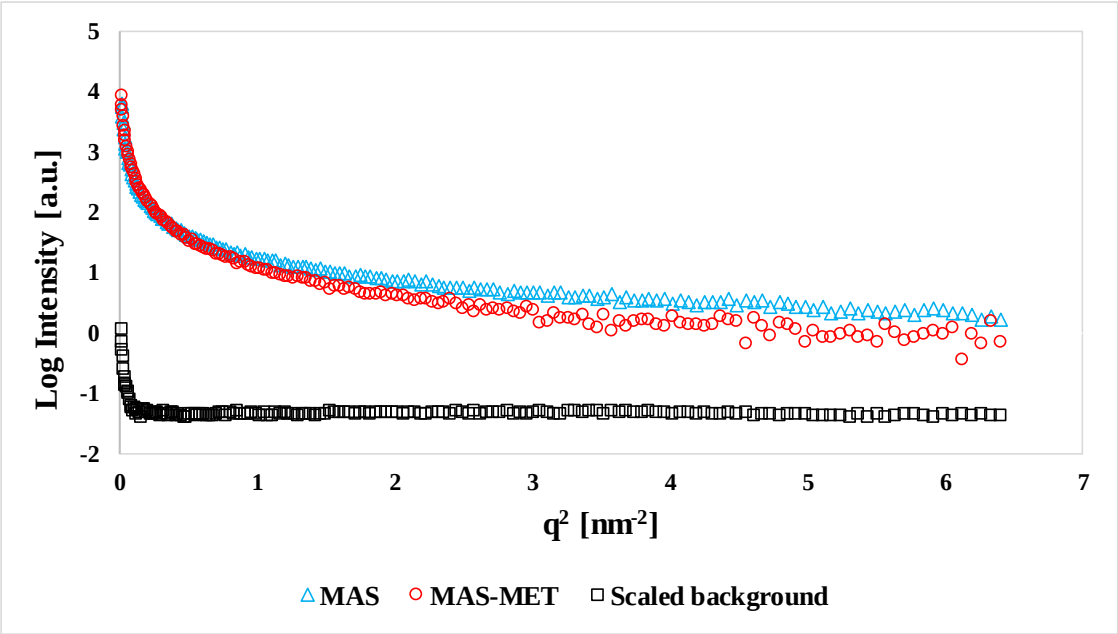

Fig 12. Guinier plot of MAS dispersion and MAS-MET complex dispersion showing two linear regions in the high and low q values

The analysis of the data in the form of double logarithmic plot of intensity (log I [a.u.]) vs. the scattering vector (log {q [nm^{-1}]}) for the MAS-MET flocculates followed straight lines with no peaks or other specific features, indicating power-law scattering behaviour (Fig 13.). This behaviour was also observed following the analysis of the MAS dispersion.

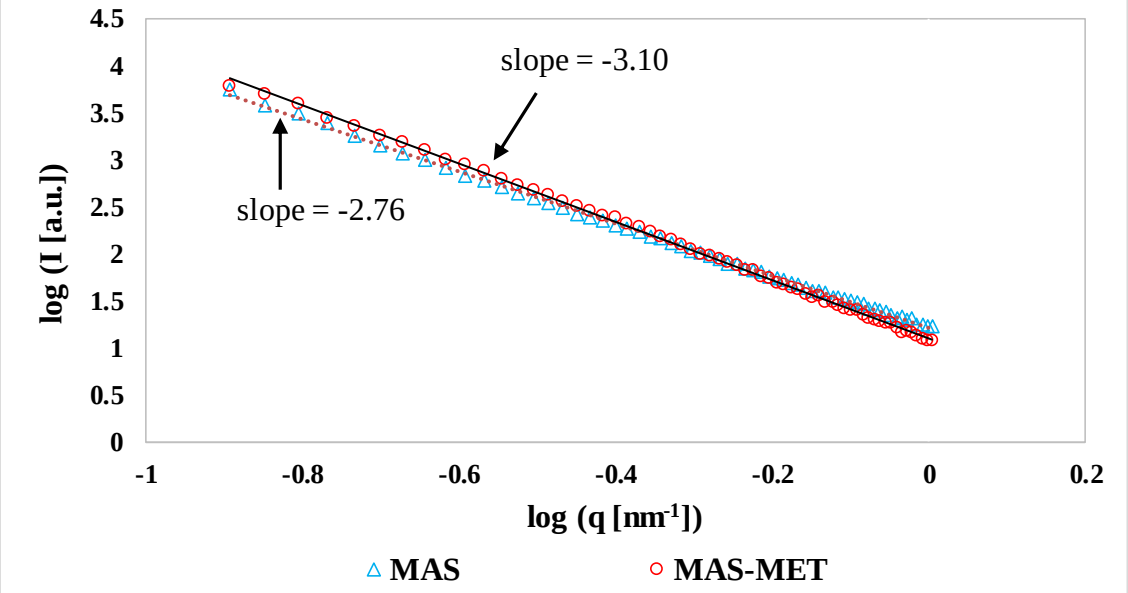

Fig 13. Double-logarithmic plot of intensity vs. the scattering vector for MAS and MAS-MET complexes in liquid form, showing power law behaviour

A slope of – 3.10 was obtained for the MAS-MET complex dispersion, which was considerably different from the one obtained for MAS (– 2.76). The difference in results shows a difference in structure, with the MAS-MET complex dispersion having a more complex structure. This behaviour was expected since the MAS flocculated upon the addition of the MET solution.

3.7. High Performance Liquid Chromatography (HPLC)

3.7.1. Method validation

The calibration curve generated for the MET using pure drug solutions dissolved in water was found to be linear over the concentration range studied ($R^2 \geq 0.999$). Linearity was defined by an equation (y = 92162 x + 17244). This equation was further used in the MET recovery studies. The intermediate and intra assay precision at three different concentration levels of 10, 50 and 100 µg/mL ranging from 0.09 % to 0.72 % and from 0.25 % to 1.72 % respectively proved the method to be precise for the detection of MET. This was evident in the lower than 2 % RSD

which complies with the acceptable criteria for quality control of pharmaceutical preparations.[31], [32] The LOQ showing the lowest drug concentration that can be recovered within acceptable limits of precision and accuracy was found to be 1.01 µg/mL indicating the high sensitivity of the proposed method and its suitability for the detection MET in solutions at low concentrations. LOD showing the lowest detectable amount of drug distinguishable from the blank was 0.33 µg/mL also showing the sensitivity of the method (Table 2).

Table 2. HPLC method validation for MET showing linearity range, intermediate and intra assay precision, LOD and LOQ.

Range (µg/mL)	**Linearity (R^2)**	**Intermediate precision (RSD) (%)**	**Intra assay precision (RSD) (%)**	**LOD (µg/mL)**	**LOQ (µg/mL)**
100 – 0.1	≥ 0.9999	1 µg/mL: 2.68 10 µg/mL: 1.72 50 µg/mL: 0.97 100 µg/mL: 0.69	1 µg/mL: 1.85 10 µg/mL: 0.72 50 µg/mL: 0.71 100 µg/mL:0.24	0.33	1.01

3.7.2. Determination of drug content in MAS – drug complex particles

Determination of MET content in the MAS-MET complex particles prepared showed differences between the different media used for the dispersion of the complex particles (2 M HCl, pH 5 ultra-pure water and pH 6.8 buffer) (Table 3.).

Table 3. MET content in MAS–MET complex particles using three different dissolution media: 2M HCl, ultra-pure water (pH 5) and phosphate buffer (pH 6.8).

	Recovered MET (% w/w)
	MAS-MET double drug loaded
2M HCl	8.75 ± 0.14*
pH 5.0 Ultra-pure water	1.31 ± 0.06*

pH 6.8 Phosphate Buffer	1.60 ± 0.08*

Note: *values are reported as the mean ± SD of at least three determinations

MET is a highly stable drug with two pK_a values, 2.8 and 11.5 and an aqueous solubility of 300 mg/mL in the pH range 1.2 – 6.8.[33] Hence, the amount of MET recovered from the MAS – MET complex particles dispersed in 2 M HCl, ultra – pure water and pH 6.8 phosphate buffer should be pH independent. However, the amount of MET recovered was highly variable (Table 3). No degradation products were however observed on the chromatograms during the analysis in any of the dissolution media used.

3.8. Calorimetric binding studies

3.8.1. Calorimetric single injection (SIM) binding studies

The interaction between MAS and MET was initially studied using ITC SIM experiments (Fig 14.). The experiments confirmed the binding between MET solution (0.016 % w/v) and MAS dispersion (0.010 % w/v), which was shown to be exothermic at the pH values investigated. The binding was faster and more exothermic at pH 5, as shown by the larger peak returning faster to the baseline compared to the peaks observed in the ITC experiments at pH 7 and 9 (Fig 14.). Further work therefore focused on multiple injection experiments (MIM) to explore the adsorption of MET onto MAS at pH 5.

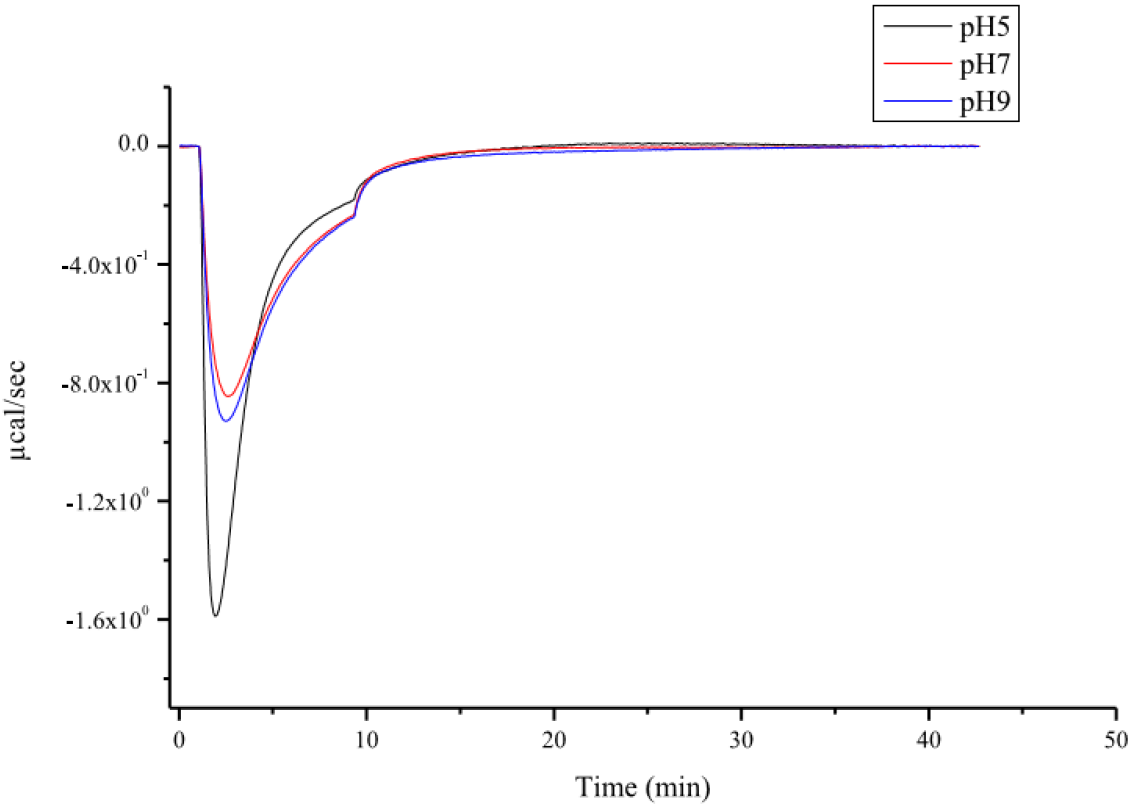

Fig 14. Titration of 0.016 % w/v (1 mM) MET solution (pH 5) into 0.010 % w/v MAS dispersion pH 5 (black), pH 7 (red) and pH 9 (green) at 25 °C

3.8.2. Calorimetric multiple injection mode (MIM) binding studies

MIM ITC experiments at pH 5 and at two different temperatures (25 and 37 °C) further confirmed the highly exothermic interaction between MET and MAS (Fig 15.) as previously observed in the SIM ITC experiments. The MIM stepwise experiments however gave more detailed information about the driving forces involved in the process of adsorption of MET onto MAS. In order to determine the heat of dilution for MAS and MET, the subtraction of the heat of dilution for MET (0.033 % w/v (pH 5)) and water (pH 5) was required for both experiments at 25 and 37 ºC (Fig 15.). A one set of sites model was fitted to the data and allowed the determination of thermodynamic parameters of the reaction: affinity (K_a), changes in enthalpy (ΔH), entropy (ΔS) or Gibbs free energy (ΔG).

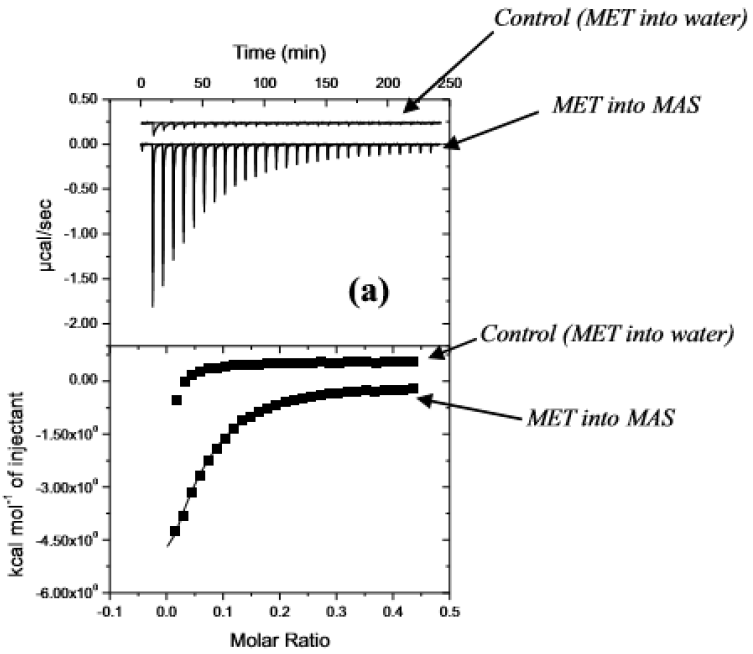

480

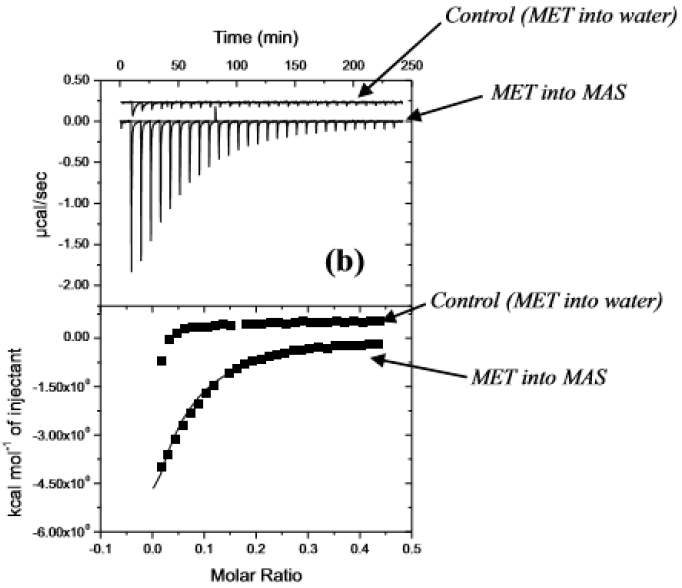

481

482 **Fig 15.** Multiple injection mode calorimetric titration of 0.033 % w/v MET solution (pH 5)
483 into 0.037 % w/v MAS dispersion (pH 5) at 25 °C (a) and 37 °C (b). Raw data (top) and
484 integrated heats (bottom) as a function of molar ratio. Control runs suggesting interaction
485 between water and MET

Binding was characterised by a negative enthalpy change, and a comparatively small entropy change at both 25 and 37 °C, implying that the binding was an enthalpically driven process (Fig 16.).

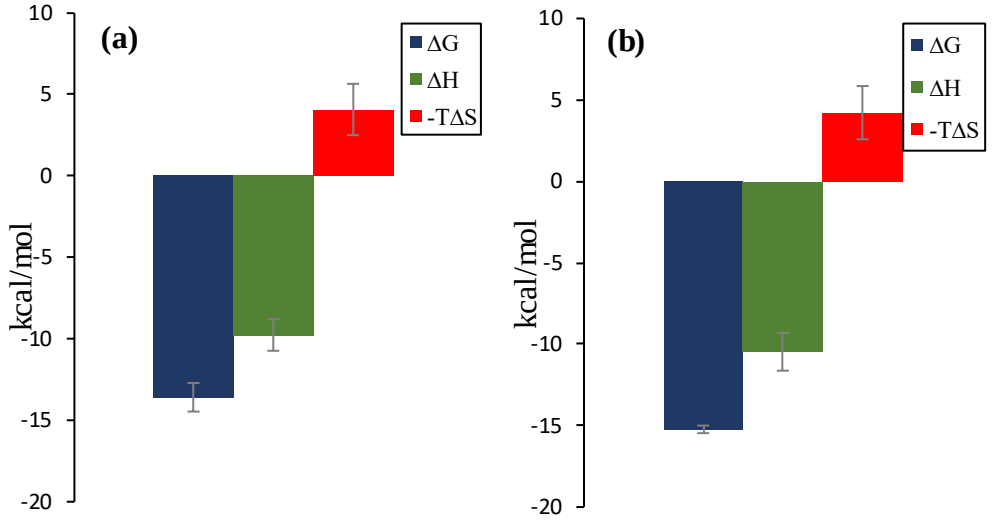

Fig 16. Thermodynamic profile for binding of MET (0.033 % w/v) onto MAS (0.037 % w/v) at 25 °C (a) and 37 °C (b) showing enthalpy (ΔH), entropy(ΔS) or Gibbs free energy (ΔG). Results are based on three independent repeats done under similar conditions.

The increase in temperature caused a gradual increase in the affinity of MET with MAS as observed from the increase of the association constant K_a (1.47E+04 ± 2.06E+03 M at 25 °C and 4.66E+04 ± 1.2E+04 at 37 °C) (Table 4.). The overall change in Gibbs free energy (ΔG) was comparatively similar at both temperatures (-12.11 ± 4.04 kcal/mol at 25 °C compared with -14.69 ± 1.01 kcal/mol at 37 °C), confirming that both reactions occurred spontaneously. The enthalpic contribution calculated from the change in heat associated with binding was slightly greater at 37 °C (-8.81 ± 2.52 kcal/mol at 25 °C compared with -10.47 ± 1.61 kcal/mol at 37 °C), while the entropic contribution was comparatively small in both cases confirming the interaction to be enthalpically driven at both temperatures. The binding interaction had a negative heat capacity ΔCp (-0.14 kcal mol K^{-1}) indicating that upon increasing temperature, the binding became more exothermic and enthalpically driven, thus in agreement with the

binding parameters calculated. The values calculated for the thermodynamic parameters from the ITC experiments suggest an exothermic interaction and good hydrogen bonding. MET is therefore expected to be adsorbed onto MAS through the amine groups which allows cation exchange, as well as hydrogen bonding and water bridging (Fig 17.).

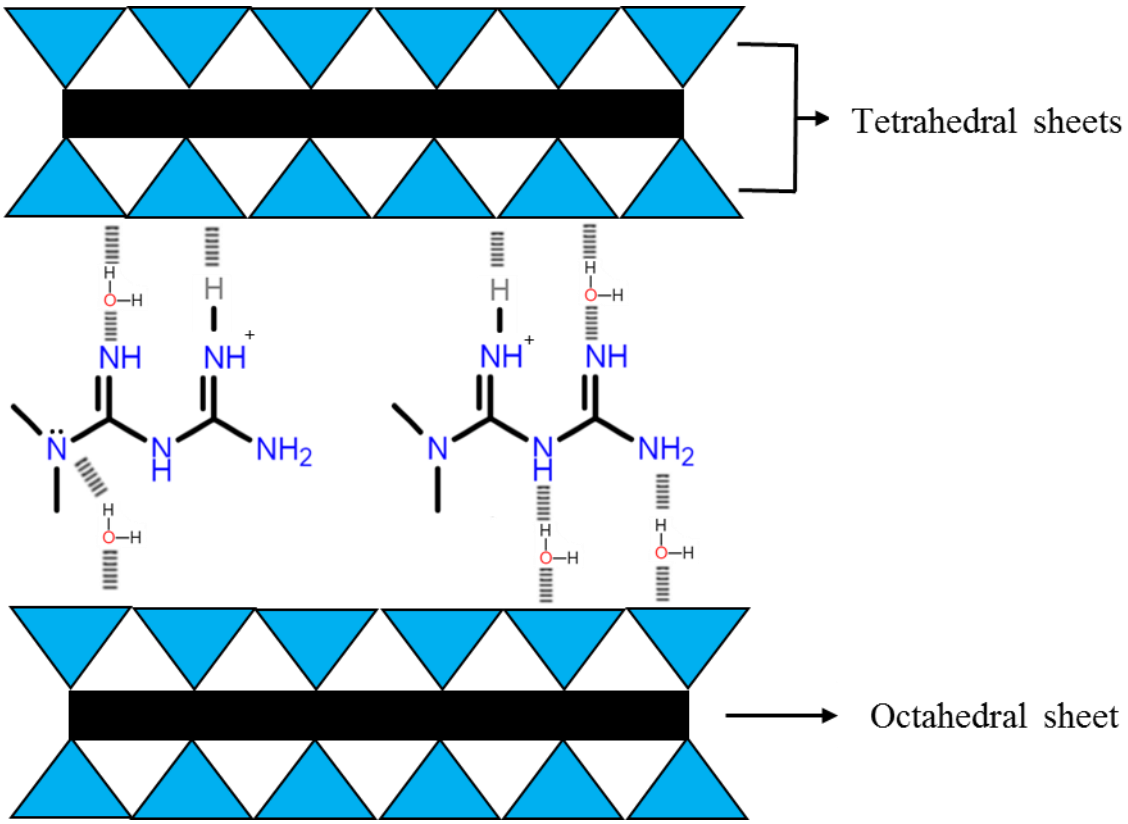

Fig 17. Possible MAS-MET chemical interaction: cation exchange, hydrogen bonding and water bridging

4. Conclusion:

ITC was successfully used in understanding the complexation process occurring between magnesium aluminium silicate (MAS) and (MET), as a potential controlled release drug delivery system. The calorimetric studies revealed that the binding was an enthalpically driven process, dominated by hydrogen bonding and electrostatic interactions. Changes in enthalpy (ΔH), entropy (ΔS) and Gibbs free energy (ΔG) were similar at the pHs and temperatures explored in experiments with the reaction being only slightly more exothermic at pH 5 and at 37 °C. MAS and MET complex dispersions and particles were also formulated and analysed

successfully using DSC, XRPD, ATR-FTIR, SEM/EDX, digital microscopy and 2D-SAXS. Humidity was shown to have a great impact on the basal distance determination using XRPD therefore suggesting the technique to be an inaccurate indicator of complexation between MAS and MET. 2D-SAXS on the other hand was able to differentiate between MAS particulates and MAS-MET complexes when analysed in their liquid form. Care and consideration should thus be taken in the accurate determination and characterisation techniques for the formation of complexes for controlled release.

Acknowledgements

The authors acknowledge the University of Huddersfield for financial support and for funding A.M Totea's PhD study.

Conflict of interest

The authors declare no conflict of interest

Author contributions

A. M. Totea: Conceptualisation; Data curation; Formal analysis; Methodology; Investigation Writing—Original Draft; Writing—Review & Editing;

I. Dorin; Resources; Software; Validation; Formal analysis; Methodology;

P. R. Laity; Supervision; Validation; Formal analysis; Methodology;

B. R. Conway; Supervision; Methodology;

L. Waters; Supervision; Methodology; Writing—Review & Editing;

K.Asare-Addo; Funding acquisition; Conceptualisation; Formal analysis; Methodology; Writing—Original Draft; Writing—Review & Editing; Supervision;

References

[1] A. M. Totea *et al.*, "Real time calorimetric characterisation of clay – drug complex dispersions and particles," *Int. J. Pharm. X*, vol. 1, no. December 2018, p. 100003, 2019.

[2] A. M. Totea *et al.*, "Thermodynamics of clay – Drug complex dispersions: Isothermal titration calorimetry and high-performance liquid chromatography," *J. Pharm. Anal.*, vol. 10, pp. 78–85, 2019.

[3] S. Rojtanatanya and T. Pongjanyakul, "Propranolol-magnesium aluminum silicate complex dispersions and particles: Characterization and factors influencing drug release," *Int. J. Pharm.*, vol. 383, no. 1–2, pp. 106–115, 2010.

[4] T. Pongjanyakul and S. Rojtanatanya, "Use of Propranolol-Magnesium Aluminium Silicate Intercalated Complexes as Drug Reservoirs in Polymeric Matrix Tablets," *Indian J. Pharm. Sci.*, vol. 74, no. 4, pp. 292–301, 2012.

[5] W. Khunawattanakul, S. Puttipipatkhachorn, T. Rades, and T. Pongjanyakul, "Chitosan-magnesium aluminum silicate nanocomposite films: Physicochemical characterization and drug permeability," *Int. J. Pharm.*, vol. 393, no. 1–2, pp. 220–230, 2010.

[6] A.-M. Totea *et al.*, "A molecular understanding of magnesium aluminium silicate – drug, drug – polymer, magnesium aluminium silicate – polymer nanocomposite complex interactions in modulating drug release: Towards zero order release," *Eur. J. Pharm. Biopharm.*, vol. 154, pp. 270–282, 2020.

[7] K. Asare-Addo, A.-M. Totea, and A. Nokhodchi, "Drug release from magnesium aluminium silicate-polyethylene oxide (PEO) nanocomposite matrices: An

566 investigation using the USP III apparatus," *Eur. J. Pharm. Sci.*, vol. 153, p. 105474,
567 2020.

568 [8] E. P. Rebitski, P. Aranda, M. Darder, R. Carrarob, and E. Ruiz-Hitzky, "Intercalation
569 of metformin into montmorillonite," *Dalt. Trans.*, vol. 47, pp. 3185–3192, 2018.

570 [9] W. Kanjanakawinkul, T. Rades, S. Puttipipatkhachorn, and T. Pongjanyakul,
571 "Nicotine-magnesium aluminum silicate microparticle surface modified with chitosan
572 for mucosal delivery," *Mater. Sci. Eng. C*, vol. 33, no. 3, pp. 1727–1736, 2013.

573 [10] B. K. G. Theng, *Formation and Properties of Clay-Polymer Complexes*, 2nd ed.
574 Amsterdam: Elsevier Science, 2012.

575 [11] Vanderbilt Minerals, "VEEGUM ® Magnesium Aluminum Silicate VANATURAL ®
576 Bentonite Clay For Personal Care and Pharmaceuticals What They Are," Norwalk, pp.
577 1–27, 2014.

578 [12] K. Wadher, M. Umekar, and R. Kakde, "Formulation and evaluation of a sustained-
579 release tablets of metformin hydrochloride using hydrophilic synthetic and
580 hydrophobic natural polymers," *Indian J. Pharm. Sci.*, vol. 73, no. 2, p. 208, 2011.

581 [13] M. Kinaan, H. Ding, and C. R. Triggle, "Metformin: An Old Drug for the Treatment of
582 Diabetes but a New Drug for the Protection of the Endothelium," *Med. Princ. Pract.*,
583 vol. 24, no. 5, pp. 401–415, 2015.

584 [14] G. Li, G. Srijib, G. Kathleen M., A. Russ B., and K. Teri E., "Metformin pathways:
585 pharmacokinetics and pharmacodynamics," *Pharmacogenet Genomics*, vol. 22, no. 11,
586 pp. 820–827, 2012.

587 [15] R. A. DeFronzo and A. M. Goodman, "Efficacy of Metformin in Patients With Non-
588 Insulin-Dependent Diabetes," *Multicent. Metformin Study Gr. New Engl. J. Med.*, vol.

333, no. 9, pp. 541–549, 1995.

[16] O. Defang, N. Shufang, L. Wei, G. Hong, L. Hui, and P. Weisan, "In vitro and in vivo evaluation of two extended release preparations of combination metformin and glipizide," *Drug Dev. Ind. Pharm.*, vol. 31, no. 7, pp. 677–685, 2005.

[17] A. M. Totea, I. Dorin, P. R. Laity, B. R. Conway, L. Waters, and K. Asare-addo, "Use of thermodynamics in understanding drug release from xanthan gum matrices : The influence of clay-drug complexes," *Carbohydr. Polym. Technol. Appl.*, vol. 1, p. 100012, 2020.

[18] Vanderbilt Minerals, "VEEGUM / VAN GEL Magnesium Aluminum Silicate Magnesium Aluminum Silicate ® The Story," Norwalk, 2014.

[19] J. Coates, "Interpretation of Infrared Spectra, A Practical Approach," *Encycl. Anal. Chem.*, pp. 10815–10837, 2000.

[20] MicroCal, *VP-ITC User's Manual*. Northampton, 1998.

[21] N. R. Sheela, S. Muthu, and S. S. Krishnan, "FTIR , FT Raman and UV-Visible Spectroscopic Analysis on Metformin Hydrochloride," *Asian J. Chem.*, vol. 22, no. 7, pp. 5049–5056, 2010.

[22] S. Gunasekaran, R. K. Natarajan, V. Renganayaki, and S. Natarajan, "Vibrational spectra and thermodynamic analysis of metformin," *Indian J. Pure Appl. Phys.*, vol. 44, no. 7, pp. 495–500, 2006.

[23] C. Aguzzi, P. Cerezo, C. Viseras, and C. Caramella, "Use of clays as drug delivery systems: Possibilities and limitations," *Appl. Clay Sci.*, vol. 36, no. 1–3, pp. 22–36, 2007.

[24] S. Manoranjan, "Formulation of dual component drug delivery of glimepiride and

612 metformin hydrochloride for immediate and sustain release," *Int. J. Res. Ayurveda*
613 *Pharm.*, vol. 1, no. 2, pp. 624–633, 2010.

614 [25] P. Vaingankar and P. Amin, "Continuous melt granulation to develop high drug loaded
615 sustained release tablet of Metformin HCl," *Asian J. Pharm. Sci.*, vol. 12, no. 1, pp.
616 37–50, 2017.

617 [26] S. C. Jagdale, S. A. Patil, B. S. Kuchekar, and A. R. Chabukswar, "Preparation and
618 characterization of metformin hydrochloride-compritol 888 ATO solid dispersion," *J.*
619 *Young Pharm.*, vol. 3, no. 3, pp. 197–204, 2011.

620 [27] I. H. Milne and C. M. Warhaw, "Methods of Preparation and Control of Clay Mineral
621 Specimens in X-Ray Diffraction Analysis," *Clays Clay Miner.*, vol. 4, pp. 22–30,
622 1955.

623 [28] H. Hashizume, S. Shimomura, H. Yamada, T. Fujita, and H. Nakazawa, "an X-Ray
624 Diffraction System With Controlled Relative Humidity and Temperature," vol. 14, no.
625 1, pp. 1–4, 1997.

626 [29] A. Bandyopadhyay and S. Bose, Eds., *Characterization of Biomaterials Chapter 4*.
627 Oxford, UK: Elsevier, 2013.

628 [30] E. A. Odo, D. T. Britton, G. G. Gonfa, and M. Harting, "SAXS Study of Silicon
629 Nanocomposites," vol. 5, no. 3, pp. 65–70, 2015.

630 [31] V. A. Chatpalliwar, P. K. Porwal, and N. Upmanyu, "Validated gradient stability
631 indicating HPLC method for determining Diltiazem Hydrochloride and related
632 substances in bulk drug and novel tablet formulation," *J. Pharm. Anal.*, vol. 2, no. 3,
633 pp. 226–237, 2012.

634 [32] J. Ermer and H. J. Ploss, "Validation in pharmaceutical analysis: Part II: Central

importance of precision to establish acceptance criteria and for verifying and improving the quality of analytical data," *J. Pharm. Biomed. Anal.*, vol. 37, no. 5, pp. 859–870, 2005.

[33] D. Desai *et al.*, "Surfactant-mediated dissolution of metformin hydrochloride tablets: Wetting effects versus ion pairs diffusivity," *J. Pharm. Sci.*, vol. 103, no. 3, pp. 920–926, 2014.